THE JOURNAL OF PHYSICAL CHEMISTRY B

pubs.acs.org/JPCB Article

Transition between Different Diffusion Regimes and Its Relationship with Structural Properties in Nafion by High Field Diffusion NMR in Combination with Small-Angle X-ray and Neutron Scattering

Samuel J. Berens, Ahmad Yahya, Junchuan Fang, Anastasios Angelopoulos, Jonathan D. Nickels, and Sergey Vasenkov*

Cite This: J. Phys. Chem. B 2020, 124, 8943–8950 Read Online

ACCESS | Metrics & More | Article Recommendations | Supporting Information

ABSTRACT: Pulsed field gradient (PFG) NMR at high field was utilized to directly observe a transition between two different diffusion regimes in a Nafion 117 membrane loaded with water and acetone. Although water self-diffusivity at small water loadings was observed to be diffusion time-independent in the limit of small and large diffusion times, it showed a significant decrease with increasing diffusion time at intermediate times corresponding to root mean square displacements on the order of several microns. Under our experimental conditions, no self-diffusivity dependence on diffusion time was found for water at large water loadings and for acetone at all studied acetone loadings. The diffusion time-dependent self-diffusivity at small water concentration is explained by the existence of finite domains of interconnected water channels with sizes in the range of several microns that form in Nafion in the presence of acetone. The domain sizes and permeance of transport barriers separating adjacent domains are estimated based on the measured PFG NMR data. At large water concentrations, the water channels form a fully interconnected network, resulting in time-independent self-diffusivity. The absence of such a percolation-like transition with increasing molecular concentration for acetone is attributed to a difference in the regions available for water and acetone diffusion in Nafion. The diffusion data are correlated with and supported by structural data obtained using small-angle X-ray and neutron scattering techniques. These techniques reveal distinct water channels with radial dimensions in the nanometer range increasing upon water addition, while acetone appears to be in an interfacial perfluoroether region, reducing the size of the radial channel dimension.

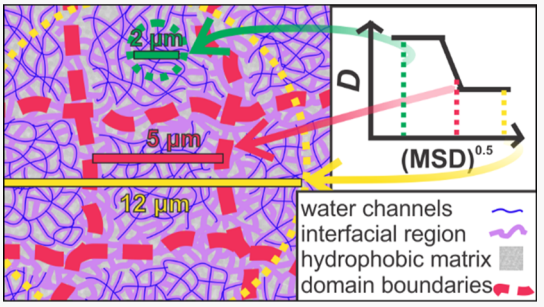

INTRODUCTION

Nafion is a commercially available perfluorinated sulfonic acid ionomer which has been well-studied for its potential or current applications in fuel cells,[1−4] water desalination processes,[5,6] and chemical sensing,[7−10] to name a few. In the presence of water, the Nafion structure exhibits a hydrophobic semicrystalline matrix made of a backbone of polytetrafluoroethylene and channels available for water diffusion, viz., water channels. These channels are formed by perfluoroalkyl ether side chains terminated by sulfonic acid groups.[11−17] At sufficiently high water concentrations, water channels can form an interconnected network allowing for fast water diffusion through an entire membrane.[14,16,18]

As Nafion can be used as a solid electrolyte membrane for either hydrogen or direct-methanol fuel cells, dynamics and transport of water and methanol within the membrane has been studied by a variety of methods including uptake/permeation measurements,[19−21] NMR,[22−29] and computer simulations.[30−32] In several microscopic diffusion studies, specifically those utilizing diffusion NMR techniques, the self-diffusivity of water in Nafion in the limit of short diffusion times was found to decrease significantly as diffusion time is increased.[27,31,33−35] At larger diffusion times, the water self-diffusivity approached constant, time-independent values. Additionally, the self-diffusion coefficient of ethanol in Nafion was found to have no dependence on diffusion time while decafluoropentane was observed to have a significant drop in self-diffusivity with increasing diffusion time.[36] The time-dependent diffusion behavior at the limit of small times is not unique to Nafion as the water diffusivity decreasing with diffusion time was also observed in similar membrane types, including sulfonated polyether sulfone[35] and polyelectrolyte−fluoropolymer blend membranes.[37]

In the previous studies, the interpretation of the observed decrease in molecular self-diffusivity with increasing diffusion time in the limit of small times usually involves a hypothesis

Received: August 7, 2020
Revised: September 14, 2020
Published: September 15, 2020

https://dx.doi.org/10.1021/acs.jpcb.0c07249
J. Phys. Chem. B 2020, 124, 8943–8950

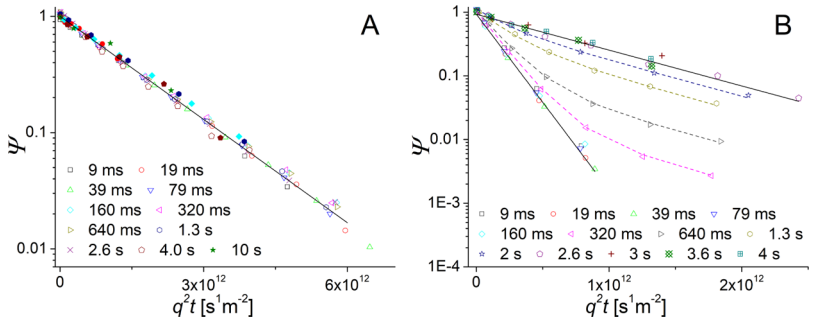

Figure 1. ^{1}H (hollow symbols) and ^{13}C (filled symbols) PFG NMR attenuation curves for acetone (A) and water (B) in a Nafion membrane at 296 K. The acetone and water concentrations in the membrane were 0.55 and 1.7 mmol/g, respectively. Solid lines represent the best fit lines using the monoexponential attenuation model (eq 1). Dashed lines represent a biexponential fit (eq 4) used for the water attenuation at intermediate diffusion times.

about the existence of finite, micrometer-sized domains in Nafion with faster molecular diffusion inside the domains and slower diffusion through the domain boundaries, that is, transport barriers, separating neighboring domains. Based on this hypothesis, a time-independent self-diffusivity can be expected at sufficiently short times when molecular displacements are much smaller than the domain sizes. As discussed above, the diffusivity approaches a time-independent value also in the limit of large times when most molecules diffused inside the domains and through the boundaries separating neighboring domains. However, to our knowledge, two diffusion regimes with time-independent self-diffusivities and a clear transition between these regimes characterized by decreasing diffusivity with increasing time were never observed in Nafion using a single technique. Herein, we report such an observation for water diffusion in the presence of acetone inside a Nafion 117 membrane. This observation was made by pulsed field gradient (PFG) NMR at a high magnetic field for the smallest water concentration in Nafion used in this study.

The interest in acetone is related to its possible use as a Nafion swelling agent to mitigate steric exclusion of reactant molecules and promote reactivity in heterogeneous catalysis applications such as biofuel production.[38−40] In addition, Nafion can be used as an extremely sensitive sensor for acetone vapor in humid environments, which can potentially be utilized in medical diagnostic procedures and other applications.[9,10] In particular, acetone in exhaled breath has been repeatedly correlated to blood biomarkers such as acetoacetate and β-hydroxybutyrate that are associated with diabetes mellitus.[41] It was recently shown that the presence of water in human breath can have significant impact on the optical response arising from the chemical reaction between reagent molecules immobilized within the Nafion membrane and acetone.[42−44] Clearly, the diffusion behavior of water and acetone in Nafion is expected to play a significant role in the catalysis and sensor applications mentioned above.

In addition to obtaining the time-independent water self-diffusivity inside the Nafion domains in the limit of small diffusion times when there is no influence from the domain boundaries, the PFG NMR technique allowed, for the first time, quantifying the permeance of the domain boundaries. The average domain size was also estimated. At larger water concentrations, the water self-diffusivities were found to be diffusion time-independent, which is consistent with the existence of fully interconnected water channels in Nafion. The acetone self-diffusivity was also found to be diffusion time-independent under all experimental conditions used. The PFG NMR diffusion data are correlated with the membrane structural data obtained by complementary small-angle X-ray (SAXS) and small-angle neutron scattering (SANS) measurements.

METHODS

Nafion Preparation. Nafion 117 (Fuel Cell Store) was purified as follows. The membrane was immersed into 5% hydrogen peroxide solution at 90 °C for 1 h to remove any impurities. Following the impurity removal, the membrane was washed with DI water and immersed into 0.5 M sulfuric acid solution at 90 °C for 1 h to fully protonate. Finally, the membrane was washed again with DI water and dried in the hood for around 12 h at ambient temperature. To prepare a Nafion sample for NMR studies, a rolled Nafion 117 membrane was placed into a thin-wall 5 mm NMR tube (Wilmad-LabGlass), which was attached to a custom-build vacuum manifold for degassing and partial water removal at 60 milliTorr and 298 K for 4 h. Desired amounts of ^{13}C-labeled acetone (Sigma-Aldrich, 99 atom % ^{13}C) and/or deionized water were added to the membrane upon degassing and partial water removal by cryogenically condensing acetone and/or water vapor from the calibrated volume of the vacuum system using liquid N_2. Upon loading, the samples were flame-sealed and left to equilibrate for at least 24 h at 298 K.

NMR. Most of the ^{1}H and ^{13}C NMR measurements were performed on a 17.6 T Bruker BioSpin wide-bore spectrometer. For PFG NMR measurements on this spectrometer, the *Diff50* diffusion probe with a GREAT60 gradient amplifier was used. Complementary ^{1}H and ^{13}C PFG NMR measurements were also performed on an AVANCE III HD narrow-bore 14 T spectrometer with a *Diff30* diffusion probe. It was verified that the diffusion data obtained using these two spectrometers were the same, within uncertainty, by measuring the same samples under the same or similar conditions. Such data agreement indicates the lack of measurement artifacts under our experimental conditions. The methods for water and acetone concentration measurements are given in the Supporting Information.

For normal diffusion with a single self-diffusivity (D), PFG NMR signal attenuation can be presented as

$$\Psi = \exp(-q^2 t D) \tag{1}$$

where $q = g\gamma_{\text{nucleus}}\delta$, g is the gradient amplitude, γ_{nucleus} is the gyromagnetic ratio for a particular nucleus, δ is the effective gradient pulse duration, and t is the diffusion time. The

https://dx.doi.org/10.1021/acs.jpcb.0c07249
J. Phys. Chem. B 2020, 124, 8943−8950

parameters used in the PFG NMR experiments are given in the Supporting Information. The values of mean square displacement (MSD) were calculated using the Einstein relation for three-dimensional diffusion

$$\langle r^2 \rangle = 6Dt \quad (2)$$

SAXS and SANS. SAXS measurements were conducted at the Advanced Photon Source in Argonne National Laboratory, beamline 12-ID-C. Measurements were taken of Nafion 117 films in sealed quartz capillaries with an incident X-ray energy of 18 keV, a sample-to-detector distance of 2.255 m, and an exposure time of 0.5 s. Data were reduced using Igor Pro and analyzed using OriginPro.

SANS measurements were conducted at the Spallation Neutron Source in Oak Ridge National Laboratory, at the EQ-SANS beamline. Measurements were made of Nafion 117 films in standard "Ti" cells with quartz windows and a 0.5 mm sample spacer. Measurements were performed with incident wavelengths of 2.5 and 10 Å and a sample-to-detector spacing of 2.5 and 4 m respectively. Data were reduced using MantidPlot and analyzed using OriginPro. Details on SAXS and SANS data processing are provided in the Supporting Information.

RESULTS AND DISCUSSION

Figure 1 shows examples of ^{1}H and ^{13}C PFG NMR attenuation curves for acetone and water in a Nafion membrane at a small water concentration of 1.7 mmol/g Nafion. The observed coincidence of the data measured for acetone with the two nuclei types (^{1}H and ^{13}C) under the same or similar conditions indicates the absence of any measurement artifacts and/or proton exchange in acetone molecules leading to transport mechanisms of these protons other than molecular diffusion. In the presentation of Figure 1, coinciding monoexponential attenuation curves indicate diffusion time-independent self-diffusivity in agreement with eq 1. Hence, the data in Figure 1A indicate that all acetone molecules diffuse with a self-diffusivity, which is the same for different diffusion times, within uncertainty. Figure 2 shows the corresponding lack of the dependence of the acetone self-diffusivity on the root MSD (rmsd) which is calculated using the Einstein relation (eq 2).

In contrast to acetone signal attenuation, the PFG NMR attenuation curves for water in Figure 1B coincide with increasing diffusion times only in the limit of short (≤160 ms) and long (≥3 s) times. The average best fits of the attenuation curves measured for the diffusion time ranges corresponding to these two limits using eq 1 are shown as solid lines in Figure 1B. The long-time attenuation curves have significantly smaller slopes than those at short times, thereby indicating a significantly lower D at larger diffusion times. At intermediate diffusion times, the initial slope of the attenuation curves changes with increasing diffusion time as they transition from short-time to long-time attenuation behavior. In this range of diffusion times, a significant deviation from the monoexponential behavior is evident. It can be attributed to the existence of more than a single ensemble of molecules diffusing with different diffusivities, as discussed below. In contrast to the low water concentration data discussed above, at larger water concentrations and in the samples without acetone, only monoexponential PFG NMR attenuation curves corresponding to the time- and displacement-independent self-diffusivities

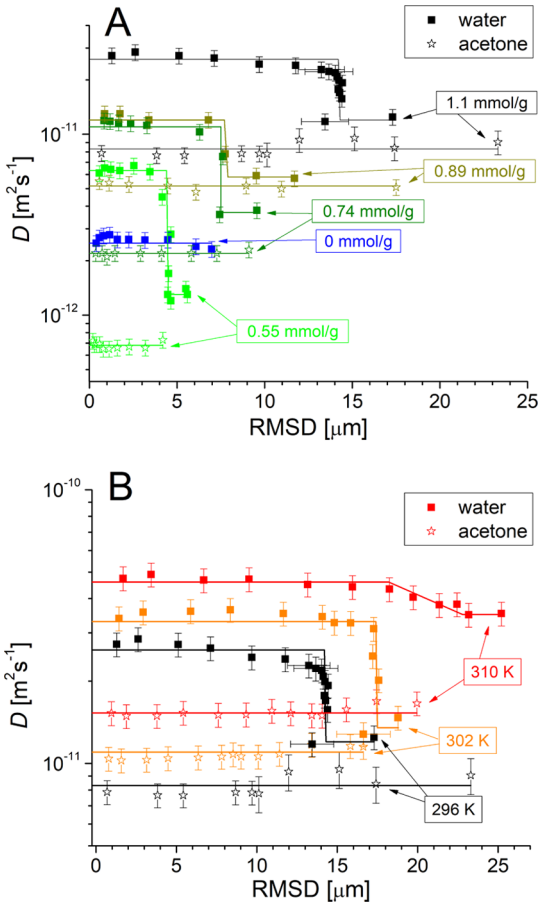

Figure 2. Dependence of the measured self-diffusivities on rmsd for acetone (star symbols) and water (square symbols) in Nafion under the following conditions: (A) varied acetone concentrations (shown with arrows) at 296 K with a constant water concentration of ∼2 mmol/g and (B) varying temperature (shown with arrows) where acetone and water concentration are held constant at ∼1 and ∼2 mmol/g, respectively. For both (A,B), solid lines are guidelines shown as visual aids. rmsds had uncertainties of around 10%, which are shown for selected points.

were observed for water in the studied Nafion samples (Figures S1 and S2).

It is well-known that in addition to the diffusion as part of water molecules, protons of water are expected to exchange in Nafion and form other diffusing species including SO_3H^+ and H_3O^+.[16] However, the proton exchange processes between all these species are expected to occur on much shorter time scales in comparison with the millisecond time scale of PFG NMR measurements.[28,34] Hence, the observed dependence of the PFG NMR diffusion data on diffusion time cannot be explained by such an exchange. Additional chemical shift and NMR relaxation data (see the Supporting Information) also point out that such an exchange does not occur on the time scale of our diffusion measurements.

To compare water self-diffusivities resulting from the data in Figure 1 across all diffusion times, we calculated a single average self-diffusion coefficient for each non-monoexponential attenuation curve using a well-established procedure,[45−48] viz., by fitting the initial parts of such attenuation curves using eq 1. Owing to the observation that the deviations from the monoexponential behavior were observed only after ∼90% of the PFG NMR signal attenuation, the initial attenuation range

https://dx.doi.org/10.1021/acs.jpcb.0c07249
J. Phys. Chem. B 2020, 124, 8943−8950

Table 1. Average Size of Domains of Interconnected Water Channels, Permeance of the Domain Boundaries, and Time Constant of Molecular Exchange for These Domains in Nafion Loaded with Acetone and Water

acetone concn (mmol/g)	H_2O concn (mmol/g)	temp. (K)	N (μm)	$P \times 10^6$ (m/s) using eq 3	R (μm)	τ_{ex} (s)	$P \times 10^6$ (m/s) using eq 5
0.55 ± 0.06	1.7 ± 0.3	296	4.3 ± 0.9	0.4 ± 0.1	2.2 ± 0.5	1.6 ± 0.2	0.5 ± 0.1
0.74 ± 0.07	2.0 ± 0.4	296	7.3 ± 1.0	0.7 ± 0.2	3.7 ± 0.5	1.6 ± 0.2	0.8 ± 0.2
0.89 ± 0.08	1.9 ± 0.4	296	7.7 ± 1.0	1.4 ± 0.4	3.9 ± 0.5	1.3 ± 0.1	1.0 ± 0.3
1.1 ± 0.1	2.2 ± 0.4	296	14 ± 2	1.5 ± 0.5	7 ± 1	1.9 ± 0.2	1.3 ± 0.4
1.0 ± 0.1	2.2 ± 0.4	302	18 ± 2	1.3 ± 0.4	9 ± 1	2.5 ± 0.5	1.2 ± 0.4
0.88 ± 0.09	1.8 ± 0.4	310	23 ± 4	5.8[a]	12 ± 2	2.0 ± 0.2	2.1[a]

[a]Large experimental uncertainty in the range of a factor of 2.

of 1.0−0.1 was used in the fitting to determine average diffusivities (Figure S3). These average self-diffusivities are shown in Figure 2 as a function of rmsd together with the corresponding self-diffusivities obtained from the monoexponential attenuation curves at smaller and larger diffusion times for the low water concentration of around 2 mmol/g. Also, as an alternative presentation, these same self-diffusivity data are plotted as a function of diffusion time in Figure S4. In Figure 2A these data are presented for different acetone concentrations, including zero acetone concentration, and approximately constant water concentration at 296 K.

Figure 2B shows the corresponding data at different temperatures and approximately constant acetone and water concentrations. It is seen in Figure 2 that the acetone self-diffusivity ($D_{acetone}$) does not change, within uncertainty, with increasing rmsd. However, the diffusion data for water in Figure 2 suggest that the water self-diffusivity (D_{water}) is independent of rmsd only at small and large rmsd values in the samples with nonzero acetone concentrations. At the intermediate rmsd values, D_{water} in such samples exhibits a significant decrease with increasing rmsd. All these diffusion data point out at the existence of micrometer-sized domains of interconnected water channels separated by areas of lower water mobility, that is, transport barriers, which can be water channel segments with a low concentration of mobile water. Such barriers are likely to be a consequence of insufficient hydration to form a fully interconnected network of water-conducting channels. Similar domains were previously suggested for Nafion,[27,33−35] although a clear and complete transition between two diffusion regimes expected for such domains was never observed. Clearly, water diffusivity is expected to decrease because of the presence of domain boundaries when the rmsd values become comparable with or larger than the domain sizes. Previously published Monte Carlo (MC) simulations show an example of the self-diffusivity dependence on rmsd for a random walk in a square lattice separated into cubic domains of equal size where the domain boundaries represent permeable transport barriers. These MC data indicate that the side length of such cubic domains (N) is approximately equal to the rmsds at the transition between the decreasing diffusivity and that reaching the lower diffusivity plateau. Using this observation and assuming the cubic shape of the domains, the average domain sizes (N) were estimated for Nafion from the data in Figure 2 and are presented in Table 1. It is important to note that the size of confining domains can, in principle, also be estimated from the diffusion time dependence of the self-diffusivity of molecules diffusing in one and the same domain.[49,50] However, this approach is well-applicable only in the limit of short times when the diffusion of the majority of molecules is not significantly affected by the domain boundaries, and the boundaries are either purely reflective or purely absorbing (i.e., molecules always leave a domain when the domain boundary is encountered). Hence, this approach of estimating the domain sizes was not used in the current study.

Table 1 shows that for small water concentration of around 2 mmol/g, the average domain size in Nafion tends to increase with increasing acetone concentration at the constant temperature of 296 K. The domain size also increases with temperature at approximately constant water and acetone concentrations of around 2 and 1 mmol/g, respectively. This behavior will be discussed later in the context of SAXS and SANS data. The permeance of the domain boundary (P) can be estimated by assuming that the overall diffusion resistance experienced by water molecules in the limit of large times can be presented as a sum of the following two resistances connected in series: resistance associated with the domain boundary permeance and the resistance associated with the intradomain diffusion[47,51]

$$\frac{1}{D_\infty} = \frac{1}{D_0} + \frac{1}{NP} \tag{3}$$

where D_0 and D_∞ denote, respectively, the time-independent self-diffusivities in the limits of small and large diffusion time measured by PFG NMR. The permeance of the domain boundary in eq 3 can be defined in complete analogy with the surface permeance as the ratio of mass flux through the boundary divided by concentration difference over the boundary. The data for the domain boundary permeance obtained using eq 3 are shown in Table 1.

The domain boundary permeance was also estimated from the measured time-dependent PFG NMR diffusion data using the PFG NMR tracer exchange approach.[47] Briefly, in this approach, the PFG NMR attenuation data for water that exhibit significant deviations from the monoexponential behavior were described assuming the existence of two molecular ensembles with different self-diffusivities (D_1 and D_∞) and the corresponding PFG NMR signal fractions (p_1 and $(1 - p_1)$)

$$\Psi = p_1 \times \exp(-q^2 t D_1) + (1 - p_1) \times \exp(-q^2 t D_\infty) \tag{4}$$

The ensemble with the larger diffusivity D_1 and the corresponding signal fraction p_1 is attributed to molecules remaining inside the same domain. The second ensemble with the signal fraction $(1 - p_1)$ was assumed to correspond to molecules diffusing with the smaller diffusivity equal to that in the long-time limit (D_∞) under the conditions of molecular exchange between different domains (see Figure 1B and Table S1 for an example of the application of eq 4). Under our experimental conditions, the PFG NMR signal fractions are expected to coincide with the corresponding molecular

https://dx.doi.org/10.1021/acs.jpcb.0c07249
J. Phys. Chem. B 2020, 124, 8943−8950

fractions of the two ensembles because there was no distribution over T_1 and T_2 relaxation times for water (see the Supporting Information for details). Hence, the fraction of molecules (γ)[47] that crossed over the domain boundary at least once and, as a result, left the original domain is expected to be equal to $(1 - p_1)$. The dependencies of $p_1 = (1 - \gamma)$ on diffusion time obtained from our PFG NMR are shown in Figure S5. The area under each of such dependencies yields the time constant of molecular exchange (τ_{ex}), that is, the mean life time of a molecule inside a given domain, which is related to the permeance of the domain boundary as[47]

$$\tau_{ex} = \int_{t=0}^{\infty} (1 - \gamma) dt = \frac{R^2}{15 D_0} + \frac{R}{3P} \quad (5)$$

where spherical domains of radius R were assumed. The values of R were estimated as $N/2$, which corresponds to equal surface-to-volume ratios for spherical and cubic domains. Using this estimate, it was found that the second term in the right-hand part of eq 5 was always much larger than the first one. This allowed estimating the values of the domain boundary permeance using eq 5 which are shown in Table 1. It is seen that within uncertainty, there is a good agreement between these values and the corresponding permeance values estimated based on eq 3. Such a coincidence confirms the validity of our permeance estimates.

The data in Table 1 show that as the concentration of acetone is increased while water concentration and temperature are held constant, P increases initially up to the acetone concentration of ~1 mmol/g after which no further increase in P is observed. Relatively large uncertainty in the values of P prevents us from making conclusions about dependence of the permeance on temperature for the same or similar water and acetone concentrations.

In order to examine a relationship of the observed diffusion properties with the corresponding structural properties, we have performed complementary SAXS and SANS measurements of Nafion loaded with acetone and water. Figure 3 shows SAXS peak positions for both the ionomer region where water channels are located (labeled ionomer/water channels) and crystalline region (labeled crystalline) in Nafion as a function of both water and acetone concentrations (see Figure S6 for primary data). The peak position in SAXS and SANS measurements describes the length scale of spatial correlations, that is, a lower q-value of a peak position (in reciprocal space) corresponds to a larger distance between two objects; such as the water channel walls[52,53] or crystalline regions.[54,55] It can be seen that the data in the upper panel of Figure 3 are consistent with an increase in the effective size of the water channel region, that is, water channel diameter increases, as the water concentration increases. In contrast, for the same water concentration, there is a clear trend of a decrease in this size with increasing acetone concentration. Additionally, SANS data also show a decrease in the effective size for the water channel region upon the addition of acetone to the Nafion membrane (Figure S7 and Table S2). All these data are indicative of added water increasing the channel diameter and added acetone reducing this diameter, which, however, remains in a nanometer range in all cases. For the crystalline region (lower panel of Figure 3), there is no clear dependence of the peak value and corresponding region's effective size on water concentration, which is in agreement with the previously published MD and SAXS studies of Nafion loaded only with water.[11,32] There is, however, a noticeable trend of an increase in the peak value with increasing acetone concentration (lower panel of Figure 3). Such an increase can be related to an accumulation of acetone within the interfacial perfluoroether regions, that is, the region between the water channel with sulfonic groups and the crystalline matrix. Indeed, such regions contribute to the distance between the neighboring crystalline segments. As a result, swelling of the interfacial perfluoroether regions with increasing acetone concentration appears to decrease the water (i.e., ionomer) channel diameter and push the crystalline regions further apart. All SAXS and SANS data discussed above indicate that acetone is likely located outside of the water channels in the interfacial perfluoroether regions. Previous SAXS studies found that with increasing methanol concentration in a methanol/water mixture, the core region of the ionomer (i.e., water channels) shrinks significantly.[56] Clearly, a similar behavior is observed here for acetone. In our opinion, it is reasonable to expect that acetone interacts with oxygen atoms of the ether groups of the pendant fluoroether side chains because of a partial negative charge on these oxygen atoms.

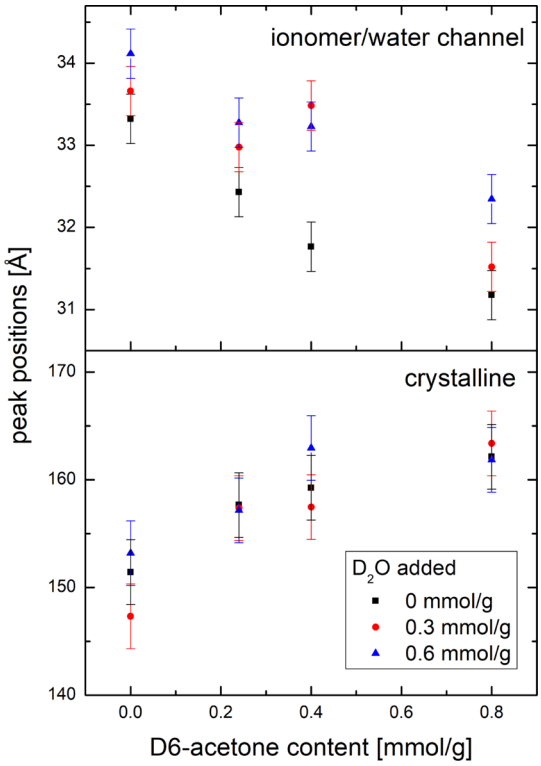

Figure 3. SAXS peak position as a function of acetone and water concentration in Nafion at 296 K. For all samples, there is an estimated additional ~0.7 mmol/g H_2O which remains in the membrane before adding D_2O and/or acetone. Therefore, the total D_2O + H_2O concentrations were 0.7, 1.0, and 1.3 mmol/g.

The preferred location of acetone in the interfacial perfluoroether regions explains why the diffusion time-dependent self-diffusivity was not observed for this molecule in the same samples where it was observed for water. It can be expected that due to acetone location outside of water channels, the channel connectivity would not play a large role in the acetone diffusion process. This is consistent with the results reported above.

Furthermore, the SAXS and SANS data discussed above can also provide a tentative explanation why the values of N

https://dx.doi.org/10.1021/acs.jpcb.0c07249
J. Phys. Chem. B 2020, 124, 8943−8950

increase with increasing acetone concentration as water concentration is held constant. If added acetone shrinks water channel diameters, some of the available water is expected to redistribute to the water channel regions with little or no mobile water. This will increase the total length of water channels with highly mobile water and, as a result, increase the size of the domains of interconnected water channels. As a consequence, the lack of the observation of the time-dependent diffusivity in the acetone-free samples with the low water concentration is likely due to the small size of the domains of interconnected water channels in these samples, that is, the domain size is smaller than the smallest measured rmsd. In addition, the observed increase in the domain boundary permeance for water diffusion with increased acetone concentration can be related to the swelling of the interfacial perfluoroether region with acetone, which is expected to make this region more permeable for water.

It is important to note that in contrast to SAXS and SANS, which provide information on the water channel diameters in the nanometer range, PFG NMR quantifies displacements because of diffusion of water molecules along the channel lengths in the micrometer range. As a result, PFG NMR allows determining properties related to channel lengths, including the sizes of water-conducting domains (viz., domains of interconnected water channels) where water molecules can freely diffuse along the channels until they encounter the domain boundaries. As discussed above, such boundaries can be formed by water channel segments with a reduced water density.

CONCLUSIONS

In summary, we report a direct PFG NMR observation of a percolation-like transition with increasing water concentration from disconnected domains of water channels to fully interconnected water channels allowing quantification of the permeance of the domain boundaries, average domain sizes, and intradomain self-diffusivity for water diffusion in Nafion loaded with both acetone and water. In contrast to the water self-diffusion, the PFG NMR self-diffusion data measured for acetone do not exhibit any evidence of finite domains with transport resistances at the domain boundaries. The complementary SAXS and SANS data suggest that acetone preferentially partitions to the interfacial perfluoroether region resulting in acetone diffusion to be insensitive to the water channel connectivity, as observed by PFG NMR. The preferential location of acetone in the interfacial perfluoroether region can also explain the observed increase in the average size of the domains and domain boundary permeance with increasing acetone concentration.

ASSOCIATED CONTENT

Supporting Information

The Supporting Information is available free of charge at https://pubs.acs.org/doi/10.1021/acs.jpcb.0c07249.

Further details on measurements of water and acetone concentration, NMR and PFG NMR measurement details, and NMR relaxation measurements; examples are shown for water PFG NMR signal attenuation in which no diffusion time dependence; details of the two-component fitting model and one-component "average" model fits of the non-monoexponential attenuation curves; examples of the diffusion time dependence of the measured self-diffusivity and the resulting data on fraction of molecules which remain in the same domain; and details of the SAXS and SANS measurements and curve fitting (PDF)

AUTHOR INFORMATION

Corresponding Author

Sergey Vasenkov − *Department of Chemical Engineering, University of Florida, Gainesville, Florida 32611, United States;* orcid.org/0000-0002-8619-0612; Phone: +1 352 392 0315; Email: svasenkov@che.ufl.edu

Authors

Samuel J. Berens − *Department of Chemical Engineering, University of Florida, Gainesville, Florida 32611, United States*

Ahmad Yahya − *Department of Chemical and Environmental Engineering, University of Cincinnati, Cincinnati, Ohio 45221, United States*

Junchuan Fang − *Department of Chemical and Environmental Engineering, University of Cincinnati, Cincinnati, Ohio 45221, United States;* orcid.org/0000-0002-7974-8788

Anastasios Angelopoulos − *Department of Chemical and Environmental Engineering, University of Cincinnati, Cincinnati, Ohio 45221, United States;* orcid.org/0000-0003-3425-9718

Jonathan D. Nickels − *Department of Chemical and Environmental Engineering, University of Cincinnati, Cincinnati, Ohio 45221, United States;* orcid.org/0000-0001-8351-7846

Complete contact information is available at: https://pubs.acs.org/10.1021/acs.jpcb.0c07249

Notes

The authors declare no competing financial interest.

ACKNOWLEDGMENTS

This research has been made possible by NSF awards nos. 1836551 and 1836556. A portion of this work was performed in the McKnight Brain Institute at the National High Magnetic Field Laboratory's Advanced Magnetic Resonance Imaging and Spectroscopy (AMRIS) Facility, which is supported by National Science Foundation Cooperative Agreement no. DMR-1644779 and the State of Florida. This work was supported in part by an NIH award, S10RR031637, for magnetic resonance instrumentation. This research used resources of the Advanced Photon Source, a U.S. Department of Energy (DOE) User Facility operated for the DOE Office of Science by Argonne National Laboratory under Contract DE-AC02-06CH11357. We would like to acknowledge Soenke Seifert for technical assistance and instrument support for SAXS experiments at Argonne National Laboratory. Research at Oak Ridge National Laboratory's Spallation Neutron Source was sponsored by the Scientific User Facilities Division, Office of Basic Energy Sciences, DOE. Oak Ridge National Laboratory facilities are sponsored by UT-Battelle, LLC, for the U.S. Department of Energy under contract no. DEAC0500OR22725. We would also like to acknowledge Changwoo Do for technical assistance and instrument support for SANS measurements at Oak Ridge National Laboratory.

REFERENCES

(1) Kreuer, K. D. On the Development of Proton Conducting Polymer Membranes for Hydrogen and Methanol Fuel Cells. *J. Membr. Sci.* **2001**, *185*, 29−39.
(2) Peighambardoust, S. J.; Rowshanzamir, S.; Amjadi, M. Review of the Proton Exchange Membranes for Fuel Cell Applications. *Int. J. Hydrogen Energy* **2010**, *35*, 9349−9384.
(3) Zhang, H.; Shen, P. K. Recent Development of Polymer Electrolyte Membranes for Fuel Cells. *Chem. Rev.* **2012**, *112*, 2780−2832.
(4) Skyllas-Kazacos, M.; Chakrabarti, M. H.; Hajimolana, S. A.; Mjalli, F. S.; Saleem, M. Progress in Flow Battery Research and Development. *J. Electrochem. Soc.* **2011**, *158*, R55.
(5) Luo, T.; Abdu, S.; Wessling, M. Selectivity of Ion Exchange Membranes: A Review. *J. Membr. Sci.* **2018**, *555*, 429−454.
(6) Sata, T.; Sata, T.; Yang, W. Studies on Cation-Exchange Membranes Having Permselectivity between Cations in Electrodialysis. *J. Membr. Sci.* **2002**, *206*, 31−60.
(7) Tailoka, F. Application of Nafion Electrolytes for the Detection of Humidity in a Corrosive Atmosphere. *Solid State Ionics* **2003**, *161*, 267−277.
(8) van der Wal, P. D.; de Rooij, N. F.; Koudelka-Hep, M. Extremely Stable Nafion Based Carbon Monoxide Sensor. *Sens. Actuators, B* **1996**, *35*, 119−123.
(9) Worrall, A. D.; Bernstein, J. A.; Angelopoulos, A. P. Portable Method of Measuring Gaseous Acetone Concentrations. *Talanta* **2013**, *112*, 26−30.
(10) Worrall, A. D.; Qian, Z.; Bernstein, J. A.; Angelopoulos, A. P. Water-Resistant Polymeric Acid Membrane Catalyst for Acetone Detection in the Exhaled Breath of Diabetics. *Anal. Chem.* **2018**, *90*, 1819−1826.
(11) Schmidt-Rohr, K.; Chen, Q. Parallel Cylindrical Water Nanochannels in Nafion Fuel-Cell Membranes. *Nat. Mater.* **2008**, *7*, 75−83.
(12) Gierke, T. D.; Munn, G. E.; Wilson, F. C. The Morphology in Nafion Perfluorinated Membrane Products, as Determined by Wide- and Small-Angle X-Ray Studies. *J. Polym. Sci., Polym. Phys. Ed.* **1981**, *19*, 1687−1704.
(13) Mauritz, K. A. Review and Critical Analyses of Theories of Aggregation in Ionomers. *J. Macromol. Sci., Polym. Rev.* **1988**, *28*, 65−98.
(14) Wescott, J. T.; Qi, Y.; Subramanian, L.; Weston Capehart, T. Mesoscale Simulation of Morphology in Hydrated Perfluorosulfonic Acid Membranes. *J. Chem. Phys.* **2006**, *124*, 134702.
(15) Yaroslavtsev, A. B. Perfluorinated Ion-Exchange Membranes. *Polym. Sci., Ser. A* **2013**, *55*, 674−698.
(16) Kusoglu, A.; Weber, A. Z. New Insights into Perfluorinated Sulfonic-Acid Ionomers. *Chem. Rev.* **2017**, *117*, 987−1104.
(17) Hiesgen, R.; Wehl, I.; Aleksandrova, E.; Roduner, E.; Bauder, A.; Friedrich, K. A. Nanoscale Properties of Polymer Fuel Cell Materials-a Selected Review. *Int. J. Energy Res.* **2010**, *34*, 1223−1238.
(18) Elliott, J. A.; Wu, D.; Paddison, S. J.; Moore, R. B. A Unified Morphological Description of Nafion Membranes from Saxs and Mesoscale Simulations. *Soft Matter* **2011**, *7*, 6820−6827.
(19) Hinatsu, J. T.; Mizuhata, M.; Takenaka, H. Water Uptake of Perfluorosulfonic Acid Membranes from Liquid Water and Water Vapor. *J. Electrochem. Soc.* **1994**, *141*, 1493.
(20) Ren, X.; Springer, T. E.; Gottesfeld, S. Water and Methanol Uptakes in Nafion Membranes and Membrane Effects on Direct Methanol Cell Performance. *J. Electrochem. Soc.* **2000**, *147*, 92−98.
(21) Balwani, A.; Davis, E. M. Anomalous, Multistage Liquid Water Diffusion and Ionomer Swelling Kinetics in Nafion and Nafion Nanocomposites. *ACS Appl. Polym. Mater.* **2019**, *2*, 40−54.
(22) Baglio, V.; Aricò, A. S.; Antonucci, V.; Nicotera, I.; Oliviero, C.; Coppola, L.; Antonucci, P. L. An Nmr Spectroscopic Study of Water and Methanol Transport Properties in Dmfc Composite Membranes: Influence on the Electrochemical Behaviour. *J. Power Sources* **2006**, *163*, 52−55.
(23) Nicotera, I.; Khalfan, A.; Goenaga, G.; Zhang, T.; Bocarsly, A.; Greenbaum, S. Nmr Investigation of Water and Methanol Mobility in Nanocomposite Fuel Cell Membranes. *Ionics* **2007**, *14*, 243−253.
(24) Ye, G.; Hayden, C. A.; Goward, G. R. Proton Dynamics of Nafion and Nafion/Sio2composites by Solid State Nmr and Pulse Field Gradient Nmr. *Macromolecules* **2007**, *40*, 1529−1537.
(25) Klein, M.; Perrin, J.-C.; Leclerc, S.; Guendouz, L.; Dillet, J.; Lottin, O. Anisotropy of Water Self-Diffusion in a Nafion Membrane under Traction. *Macromolecules* **2013**, *46*, 9259−9269.
(26) Rollet, A.-L.; Simonin, J.-P.; Turq, P.; Gebel, G.; Kahn, R.; Vandais, A.; Noël, J.-P.; Malveau, C.; Canet, D. Self-Diffusion of Ions at Different Time Scales in a Porous and Charged Medium: The Nafion Membrane. *J. Phys. Chem. B* **2001**, *105*, 4503−4509.
(27) Zhao, Q.; Majsztrik, P.; Benziger, J. Diffusion and Interfacial Transport of Water in Nafion. *J. Phys. Chem. B* **2011**, *115*, 2717−2727.
(28) Berrod, Q.; Hanot, S.; Guillermo, A.; Mossa, S.; Lyonnard, S. Water Sub-Diffusion in Membranes for Fuel Cells. *Sci. Rep.* **2017**, *7*, 8326.
(29) Zawodzinski, T. A.; Neeman, M.; Sillerud, L. O.; Gottesfeld, S. Determination of Water Diffusion Coefficients in Perfluorosulfonate Ionomeric Membranes. *J. Phys. Chem.* **1991**, *95*, 6040−6044.
(30) Hwang, G. S.; Kaviany, M.; Gostick, J. T.; Kientiz, B.; Weber, A. Z.; Kim, M. H. Role of Water States on Water Uptake and Proton Transport in Nafion Using Molecular Simulations and Bimodal Network. *Polymer* **2011**, *52*, 2584−2593.
(31) Kreuer, K.-D.; Paddison, S. J.; Spohr, E.; Schuster, M. Transport in Proton Conductors for Fuel-Cell Applications: Simulations, Elementary Reactions, and Phenomenology. *Chem. Rev.* **2004**, *104*, 4637−4678.
(32) Malek, K.; Eikerling, M.; Wang, Q.; Liu, Z.; Otsuka, S.; Akizuki, K.; Abe, M. Nanophase Segregation and Water Dynamics in Hydrated Nafion: Molecular Modeling and Experimental Validation. *J. Chem. Phys.* **2008**, *129*, 204702.
(33) Ohkubo, T.; Kidena, K.; Ohira, A. Determination of a Micron-Scale Restricted Structure in a Perfluorinated Membrane from Time-Dependent Self-Diffusion Measurements. *Macromolecules* **2008**, *41*, 8688−8693.
(34) Casieri, C.; Monaco, A.; De Luca, F. Evidence of Temperature-Induced Subdiffusion of Water on the Micrometer Scale in a Nafion Membrane. *Macromolecules* **2010**, *43*, 638−642.
(35) Ohkubo, T.; Ohira, A.; Iwadate, Y. Deconvolution and Estimation of Water Diffusion in Sulfonated Polyethersulfone Membranes Using Diffusion-Weighted Inversion Recovery. *J. Phys. Chem. Lett.* **2012**, *3*, 1030−1034.
(36) Gong, X.; Bandis, A.; Tao, A.; Meresi, G.; Wang, Y.; Inglefield, P. T.; Jones, A. A.; Wen, W.-Y. Self-Diffusion of Water, Ethanol and Decafluropentane in Perfluorosulfonate Ionomer by Pulse Field Gradient Nmr. *Polymer* **2001**, *42*, 6485−6492.
(37) Hou, J.; Li, J.; Mountz, D.; Hull, M.; Madsen, L. A. Correlating Morphology, Proton Conductivity, and Water Transport in Polyelectrolyte-Fluoropolymer Blend Membranes. *J. Membr. Sci.* **2013**, *448*, 292−299.
(38) Lopez, D.; Goodwinjr, J.; Bruce, D. Transesterification of Triacetin with Methanol on Nafion Acid Resins. *J. Catal.* **2007**, *245*, 381−391.
(39) Corain, B.; Zecca, M.; Jeřábek, K. Catalysis and Polymer Networks — the Role of Morphology and Molecular Accessibility. *Mol. Catal.* **2001**, *177*, 3−20.
(40) Krueger, A.; Balcerowiak, W.; Grzywa, E. Reasons for Deactivation of Unpromoted Polymeric Catalysts in Bisphenol a Synthesis. *React. Funct. Polym.* **2000**, *45*, 11−18.
(41) Saasa, V.; Beukes, M.; Lemmer, Y.; Mwakikunga, B. Blood Ketone Bodies and Breath Acetone Analysis and Their Correlations in Type 2 Diabetes Mellitus. *Diagnostics* **2019**, *9*, 224.
(42) Worrall, A. D.; Qian, Z.; Bernstein, J. A.; Angelopoulos, A. P. Water-Resistant Polymeric Acid Membrane Catalyst for Acetone Detection in the Exhaled Breath of Diabetics. *Anal. Chem.* **2018**, *90*, 1819−1826.

https://dx.doi.org/10.1021/acs.jpcb.0c07249
J. Phys. Chem. B 2020, 124, 8943−8950

(43) National Center for Biotechnology Information. PubChem Patent Summary for US-9921167-B2. https://pubchem.ncbi.nlm.nih.gov/patent/US-9921167-B2 (accessed Sept 11, 2020).
(44) Badmaarag, U.-O.; Bernstein, J. A.; Shekarriz, R.; Angelopoulos, A. P. Real-Time Optical Sensing of Exhaled Acetone Concentration Utilizing Non-Fickian Nafion Diffusion inside a Flow-through Sample Chamber. *Sens. Biosens. Res.* **2020**, *29*, 100373.
(45) Mueller, R.; Hariharan, V.; Zhang, C.; Lively, R.; Vasenkov, S. Relationship between Mixed and Pure Gas Self-Diffusion for Ethane and Ethene in Zif-8/6fda-Dam Mixed-Matrix Membrane by Pulsed Field Gradient NMR. *J. Membr. Sci.* **2016**, *499*, 12−19.
(46) Mueller, R.; Zhang, S.; Zhang, C.; Lively, R.; Vasenkov, S. Relationship between Long-Range Diffusion and Diffusion in the Zif-8 and Polymer Phases of a Mixed-Matrix Membrane by High Field Nmr Diffusometry. *J. Membr. Sci.* **2015**, *477*, 123−130.
(47) Kärger, J.; Ruthven, D. M.; Theodorou, D. N. *Diffusion in Nanoporous Materials*; Wiley-VCH Verlag GmbH & Co. KGaA: Weinheim, Germany, 2012.
(48) Berens, S.; Chmelik, C.; Hillman, F.; Kärger, J.; Jeong, H.-K.; Vasenkov, S. Ethane Diffusion in Mixed Linker Zeolitic Imidazolate Framework-7-8 by Pulsed Field Gradient Nmr in Combination with Single Crystal Ir Microscopy. *Phys. Chem. Chem. Phys.* **2018**, *20*, 23967−23975.
(49) Mitra, P. P.; Sen, P. N.; Schwartz, L. M. Short-Time Behavior of the Diffusion Coefficient as a Geometrical Probe of Porous Media. *Phys. Rev. B: Condens. Matter* **1993**, *47*, 8565−8574.
(50) Mitra, P. P.; Sen, P. N. Effects of Microgeometry and Surface Relaxation on NMR Pulsed-Field-Gradient Experiments: Simple Pore Geometries. *Phys. Rev. B: Condens. Matter* **1992**, *45*, 143−156.
(51) Tanner, J. E. Transient Diffusion in a System Partitioned by Permeable Barriers. Application to Nmr Measurements with a Pulsed Field Gradient. *J. Chem. Phys.* **1978**, *69*, 1748−1754.
(52) Kusoglu, A.; Modestino, M. A.; Hexemer, A.; Segalman, R. A.; Weber, A. Z. Subsecond Morphological Changes in Nafion During Water Uptake Detected by Small-Angle X-Ray Scattering. *ACS Macro Lett.* **2011**, *1*, 33−36.
(53) Gebel, G.; Lyonnard, S.; Mendil-Jakani, H.; Morin, A. The Kinetics of Water Sorption in Nafion Membranes: A Small-Angle Neutron Scattering Study. *J. Phys.: Condens. Matter* **2011**, *23*, 234107.
(54) Kim, M.-H.; Glinka, C. J.; Grot, S. A.; Grot, W. G. Sans Study of the Effects of Water Vapor Sorption on the Nanoscale Structure of Perfluorinated Sulfonic Acid (Nafion) Membranes. *Macromolecules* **2006**, *39*, 4775−4787.
(55) Mendil-Jakani, H.; Pouget, S.; Gebel, G.; Pintauro, P. N. Insight into the Multiscale Structure of Pre-Stretched Recast Nafion Membranes: Focus on the Crystallinity Features. *Polymer* **2015**, *63*, 99−107.
(56) Haubold, H.-G.; Vad, T.; Jungbluth, H.; Hiller, P. Nano Structure of Nafion: A Saxs Study. *Electrochim. Acta* **2001**, *46*, 1559−1563.

https://dx.doi.org/10.1021/acs.jpcb.0c07249
J. Phys. Chem. B 2020, 124, 8943−8950